

AD-A169 325

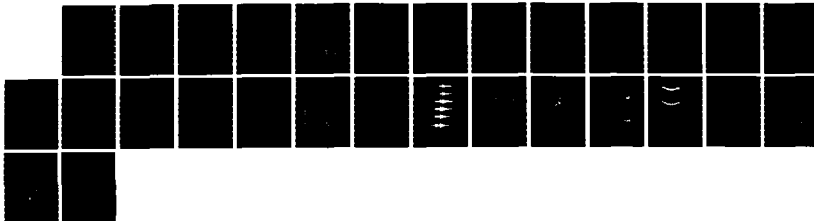
LG WAVE EXCITATION AND PROPAGATION IN PRESENCE OF ONE-
TWO- AND THREE-DIMENSIONAL HETEROGENEITIES(U) SAINT
LOUIS UNIV MO R B HERRMANN 01 FEB 86 AFGL-TR-86-0026
F19628-85-K-0029

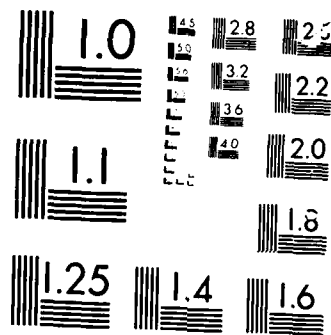
1/1

UNCLASSIFIED

F/G 8/11

NL





MICROCOPY

11-11

AD-A169 325

12

AFGL-TR-86-0026

Lg Wave Excitation and Propagation in
Presence of One-, Two-, and Three-Dimensional
Heterogeneities

R. B. Herrmann

St. Louis University
221 North Grand Blvd
St. Louis, MO 63103

1 February 1986

Scientific Report No. 2

APPROVED FOR PUBLIC RELEASE; DISTRIBUTION UNLIMITED

DTIC
ELECTE
JUL 1 1986
S B

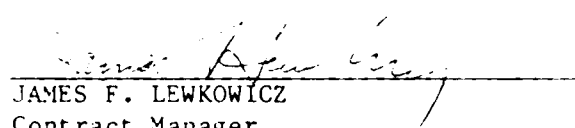
AIR FORCE GEOPHYSICS LABORATORY
AIR FORCE SYSTEMS COMMAND
UNITED STATES AIR FORCE
HANSCOM AIR FORCE BASE, MASSACHUSETTS 01731

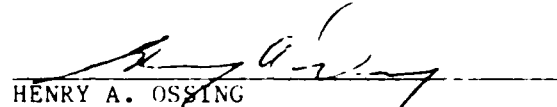
DTIC FILE COPY

86 7 1 06 9

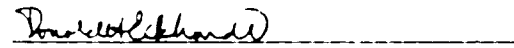
CONTRACTOR REPORTS

This technical report has been reviewed and is approved for publication.


JAMES F. LEWKOWICZ
Contract Manager


HENRY A. OSSING
Chief, Solid Earth Geophysics Branch

FOR THE COMMANDER


DONALD H. ECKHARDT
Director
Earth Sciences Division

This report has been reviewed by the ESD Public Affairs Office (PA) and is releasable to the National Technical Information Service (NTIS).

Qualified requesters may obtain additional copies from the Defense Technical Information Center. All others should apply to the National Technical Information Service.

If your address has changed, or if you wish to be removed from the mailing list, or if the addressee is no longer employed by your organization, please notify AFGL/DAA, Hanscom AFB, MA 01731. This will assist us in maintaining a current mailing list.

REPORT DOCUMENTATION PAGE

1a. REPORT SECURITY CLASSIFICATION unclassified			1b. RESTRICTIVE MARKINGS	
2a. SECURITY CLASSIFICATION AUTHORITY			3. DISTRIBUTION/AVAILABILITY OF REPORT Approved for public release. Distribution unlimited.	
2b. DECLASSIFICATION/DOWNGRADING SCHEDULE				
4. PERFORMING ORGANIZATION REPORT NUMBER(S)			5. MONITORING ORGANIZATION REPORT NUMBER(S) AFGL-TR-86-0026	
6a. NAME OF PERFORMING ORGANIZATION Saint Louis University		6b. OFFICE SYMBOL (If applicable)	7a. NAME OF MONITORING ORGANIZATION Air Force Geophysics Laboratory	
6c. ADDRESS (City, State and ZIP Code) 221 North Grand Boulevard St. Louis, MO 63103			7b. ADDRESS (City, State and ZIP Code) Hanscom Air Force Base, MA 01731	
8a. NAME OF FUNDING/SPONSORING ORGANIZATION DARPA/DSO		8b. OFFICE SYMBOL (If applicable) GSD	9. PROCUREMENT INSTRUMENT IDENTIFICATION NUMBER F19628-85-K-0029	
8c. ADDRESS (City, State and ZIP Code) 1400 Wilson Blvd. Arlington, VA 22209			10. SOURCE OF FUNDING NOS.	
			PROGRAM ELEMENT NO. 61101F	PROJECT NO. 5A10
11. TITLE (Include Security Classification) Lg Wave Excitation and Propagation (OVER)				
12. PERSONAL AUTHOR(S) R.B. Herrmann				
13a. TYPE OF REPORT Scientific Report 2		13b. TIME COVERED FROM 10/1/85 TO 3/31/86		14. DATE OF REPORT (Yr., Mo., Day) 86 FEB 01
15. PAGE COUNT 26				
16. SUPPLEMENTARY NOTATION				
17. COSATI CODES			18. SUBJECT TERMS (Continue on reverse if necessary and identify by block number) Lg attenuation and source estimates	
FIELD	GROUP	SUB GR.		
19. ABSTRACT (Continue on reverse if necessary and identify by block number) A detailed study of Lg wave excitation and propagation from a sequence of earthquakes in New Brunswick is performed. Primary conclusions are that Lg Q increases with frequency. Perhaps more importantly for regional source studies is the observation of significant high frequency Pn and Sn arrivals at 1000 km which are much greater than the Lg arrival. Source estimates based on the Lg provide reasonable estimates of seismic moment, but corner frequencies differ from short distance measurements.				
20. DISTRIBUTION AVAILABILITY OF ABSTRACT UNCLASSIFIED/UNLIMITED <input type="checkbox"/> SAME AS RPT. <input checked="" type="checkbox"/> DTIC USERS <input type="checkbox"/>			21. ABSTRACT SECURITY CLASSIFICATION Unclassified	
22a. NAME OF RESPONSIBLE INDIVIDUAL James F. Lewkowicz			22b. TELEPHONE NUMBER (Include Area Code) (617) 377-3028	22c. OFFICE SYMBOL AFGL/LWH

Cont. of Block 11:

in Presence of One-, Two-, and Three-Dimensional Heterogeneities



100-101-102
103-104-105
106-107-108
109-110-111
112-113-114
115-116-117
118-119-120
121-122-123
124-125-126
127-128-129
130-131-132
133-134-135
136-137-138
139-140-141
142-143-144
145-146-147
148-149-150
151-152-153
154-155-156
157-158-159
160-161-162
163-164-165
166-167-168
169-170-171
172-173-174
175-176-177
178-179-180
181-182-183
184-185-186
187-188-189
190-191-192
193-194-195
196-197-198
199-200-201
202-203-204
205-206-207
208-209-210
211-212-213
214-215-216
217-218-219
220-221-222
223-224-225
226-227-228
229-230-231
232-233-234
235-236-237
238-239-240
241-242-243
244-245-246
247-248-249
250-251-252
253-254-255
256-257-258
259-260-261
262-263-264
265-266-267
268-269-270
271-272-273
274-275-276
277-278-279
280-281-282
283-284-285
286-287-288
289-290-291
292-293-294
295-296-297
298-299-300
301-302-303
304-305-306
307-308-309
310-311-312
313-314-315
316-317-318
319-320-321
322-323-324
325-326-327
328-329-330
331-332-333
334-335-336
337-338-339
340-341-342
343-344-345
346-347-348
349-350-351
352-353-354
355-356-357
358-359-360
361-362-363
364-365-366
367-368-369
370-371-372
373-374-375
376-377-378
379-380-381
382-383-384
385-386-387
388-389-390
391-392-393
394-395-396
397-398-399
400-401-402
403-404-405
406-407-408
409-410-411
412-413-414
415-416-417
418-419-420
421-422-423
424-425-426
427-428-429
430-431-432
433-434-435
436-437-438
439-440-441
442-443-444
445-446-447
448-449-450
451-452-453
454-455-456
457-458-459
460-461-462
463-464-465
466-467-468
469-470-471
472-473-474
475-476-477
478-479-480
481-482-483
484-485-486
487-488-489
490-491-492
493-494-495
496-497-498
499-500-501
502-503-504
505-506-507
508-509-510
511-512-513
514-515-516
517-518-519
520-521-522
523-524-525
526-527-528
529-530-531
532-533-534
535-536-537
538-539-540
541-542-543
544-545-546
547-548-549
550-551-552
553-554-555
556-557-558
559-560-561
562-563-564
565-566-567
568-569-570
571-572-573
574-575-576
577-578-579
580-581-582
583-584-585
586-587-588
589-590-591
592-593-594
595-596-597
598-599-600
601-602-603
604-605-606
607-608-609
610-611-612
613-614-615
616-617-618
619-620-621
622-623-624
625-626-627
628-629-630
631-632-633
634-635-636
637-638-639
640-641-642
643-644-645
646-647-648
649-650-651
652-653-654
655-656-657
658-659-660
661-662-663
664-665-666
667-668-669
670-671-672
673-674-675
676-677-678
679-680-681
682-683-684
685-686-687
688-689-690
691-692-693
694-695-696
697-698-699
700-701-702
703-704-705
706-707-708
709-710-711
712-713-714
715-716-717
718-719-720
721-722-723
724-725-726
727-728-729
730-731-732
733-734-735
736-737-738
739-740-741
742-743-744
745-746-747
748-749-750
751-752-753
754-755-756
757-758-759
760-761-762
763-764-765
766-767-768
769-770-771
772-773-774
775-776-777
778-779-780
781-782-783
784-785-786
787-788-789
790-791-792
793-794-795
796-797-798
799-800-801
802-803-804
805-806-807
808-809-810
811-812-813
814-815-816
817-818-819
820-821-822
823-824-825
826-827-828
829-830-831
832-833-834
835-836-837
838-839-840
841-842-843
844-845-846
847-848-849
850-851-852
853-854-855
856-857-858
859-860-861
862-863-864
865-866-867
868-869-870
871-872-873
874-875-876
877-878-879
880-881-882
883-884-885
886-887-888
889-890-891
892-893-894
895-896-897
898-899-900
901-902-903
904-905-906
907-908-909
910-911-912
913-914-915
916-917-918
919-920-921
922-923-924
925-926-927
928-929-930
931-932-933
934-935-936
937-938-939
940-941-942
943-944-945
946-947-948
949-950-951
952-953-954
955-956-957
958-959-960
961-962-963
964-965-966
967-968-969
970-971-972
973-974-975
976-977-978
979-980-981
982-983-984
985-986-987
988-989-990
991-992-993
994-995-996
997-998-999
1000-1001-1002
1003-1004-1005
1006-1007-1008
1009-1010-1011
1012-1013-1014
1015-1016-1017
1018-1019-1020
1021-1022-1023
1024-1025-1026
1027-1028-1029
1030-1031-1032
1033-1034-1035
1036-1037-1038
1039-1040-1041
1042-1043-1044
1045-1046-1047
1048-1049-1050
1051-1052-1053
1054-1055-1056
1057-1058-1059
1060-1061-1062
1063-1064-1065
1066-1067-1068
1069-1070-1071
1072-1073-1074
1075-1076-1077
1078-1079-1080
1081-1082-1083
1084-1085-1086
1087-1088-1089
1090-1091-1092
1093-1094-1095
1096-1097-1098
1099-1100-1101
1102-1103-1104
1105-1106-1107
1108-1109-1110
1111-1112-1113
1114-1115-1116
1117-1118-1119
1120-1121-1122
1123-1124-1125
1126-1127-1128
1129-1130-1131
1132-1133-1134
1135-1136-1137
1138-1139-1140
1141-1142-1143
1144-1145-1146
1147-1148-1149
1150-1151-1152
1153-1154-1155
1156-1157-1158
1159-1160-1161
1162-1163-1164
1165-1166-1167
1168-1169-1170
1171-1172-1173
1174-1175-1176
1177-1178-1179
1180-1181-1182
1183-1184-1185
1186-1187-1188
1189-1190-1191
1192-1193-1194
1195-1196-1197
1198-1199-1200
1201-1202-1203
1204-1205-1206
1207-1208-1209
1210-1211-1212
1213-1214-1215
1216-1217-1218
1219-1220-1221
1222-1223-1224
1225-1226-1227
1228-1229-1230
1231-1232-1233
1234-1235-1236
1237-1238-1239
1240-1241-1242
1243-1244-1245
1246-1247-1248
1249-1250-1251
1252-1253-1254
1255-1256-1257
1258-1259-1260
1261-1262-1263
1264-1265-1266
1267-1268-1269
1270-1271-1272
1273-1274-1275
1276-1277-1278
1279-1280-1281
1282-1283-1284
1285-1286-1287
1288-1289-1290
1291-1292-1293
1294-1295-1296
1297-1298-1299
1300-1301-1302
1303-1304-1305
1306-1307-1308
1309-1310-1311
1312-1313-1314
1315-1316-1317
1318-1319-1320
1321-1322-1323
1324-1325-1326
1327-1328-1329
1330-1331-1332
1333-1334-1335
1336-1337-1338
1339-1340-1341
1342-1343-1344
1345-1346-1347
1348-1349-1350
1351-1352-1353
1354-1355-1356
1357-1358-1359
1360-1361-1362
1363-1364-1365
1366-1367-1368
1369-1370-1371
1372-1373-1374
1375-1376-1377
1378-1379-1380
1381-1382-1383
1384-1385-1386
1387-1388-1389
1390-1391-1392
1393-1394-1395
1396-1397-1398
1399-1400-1401
1402-1403-1404
1405-1406-1407
1408-1409-1410
1411-1412-1413
1414-1415-1416
1417-1418-1419
1420-1421-1422
1423-1424-1425
1426-1427-1428
1429-1430-1431
1432-1433-1434
1435-1436-1437
1438-1439-1440
1441-1442-1443
1444-1445-1446
1447-1448-1449
1450-1451-1452
1453-1454-1455
1456-1457-1458
1459-1460-1461
1462-1463-1464
1465-1466-1467
1468-1469-1470
1471-1472-1473
1474-1475-1476
1477-1478-1479
1480-1481-1482
1483-1484-1485
1486-1487-1488
1489-1490-1491
1492-1493-1494
1495-1496-1497
1498-1499-1500
1501-1502-1503
1504-1505-1506
1507-1508-1509
1510-1511-1512
1513-1514-1515
1516-1517-1518
1519-1520-1521
1522-1523-1524
1525-1526-1527
1528-1529-1530
1531-1532-1533
1534-1535-1536
1537-1538-1539
1540-1541-1542
1543-1544-1545
1546-1547-1548
1549-1550-1551
1552-1553-1554
1555-1556-1557
1558-1559-1560
1561-1562-1563
1564-1565-1566
1567-1568-1569
1570-1571-1572
1573-1574-1575
1576-1577-1578
1579-1580-1581
1582-1583-1584
1585-1586-1587
1588-1589-1590
1591-1592-1593
1594-1595-1596
1597-1598-1599
1600-1601-1602
1603-1604-1605
1606-1607-1608
1609-1610-1611
1612-1613-1614
1615-1616-1617
1618-1619-1620
1621-1622-1623
1624-1625-1626
1627-1628-1629
1630-1631-1632
1633-1634-1635
1636-1637-1638
1639-1640-1641
1642-1643-1644
1645-1646-1647
1648-1649-1650
1651-1652-1653
1654-1655-1656
1657-1658-1659
1660-1661-1662
1663-1664-1665
1666-1667-1668
1669-1670-1671
1672-1673-1674
1675-1676-1677
1678-1679-1680
1681-1682-1683
1684-1685-1686
1687-1688-1689
1690-1691-1692
1693-1694-1695
1696-1697-1698
1699-1700-1701
1702-1703-1704
1705-1706-1707
1708-1709-1710
1711-1712-1713
1714-1715-1716
1717-1718-1719
1720-1721-1722
1723-1724-1725
1726-1727-1728
1729-1730-1731
1732-1733-1734
1735-1736-1737
1738-1739-1740
1741-1742-1743
1744-1745-1746
1747-1748-1749
1750-1751-1752
1753-1754-1755
1756-1757-1758
1759-1760-1761
1762-1763-1764
1765-1766-1767
1768-1769-1770
1771-1772-1773
1774-1775-1776
1777-1778-1779
1780-1781-1782
1783-1784-1785
1786-1787-1788
1789-1790-1791
1792-1793-1794
1795-1796-1797
1798-1799-1800
1801-1802-1803
1804-1805-1806
1807-1808-1809
1810-1811-1812
1813-1814-1815
1816-1817-1818
1819-1820-1821
1822-1823-1824
1825-1826-1827
1828-1829-1830
1831-1832-1833
1834-1835-1836
1837-1838-1839
1840-1841-1842
1843-1844-1845
1846-1847-1848
1849-1850-1851
1852-1853-1854
1855-1856-1857
1858-1859-1860
1861-1862-1863
1864-1865-1866
1867-1868-1869
1870-1871-1872
1873-1874-1875
1876-1877-1878
1879-1880-1881
1882-1883-1884
1885-1886-1887
1888-1889-1890
1891-1892-1893
1894-1895-1896
1897-1898-1899
1900-1901-1902
1903-1904-1905
1906-1907-1908
1909-1910-1911
1912-1913-1914
1915-1916-1917
1918-1919-1920
1921-1922-1923
1924-1925-1926
1927-1928-1929
1930-1931-1932
1933-1934-1935
1936-1937-1938
1939-1940-1941
1942-1943-1944
1945-1946-1947
1948-1949-1950
1951-1952-1953
1954-1955-1956
1957-1958-1959
1960-1961-1962
1963-1964-1965
1966-1967-1968
1969-1970-1971
1972-1973-1974
1975-1976-1977
1978-1979-1980
1981-1982-1983
1984-1985-1986
1987-1988-1989
1990-1991-1992
1993-1994-1995
1996-1997-1998
1999-2000-2001
2002-2003-2004
2005-2006-2007
2008-2009-2010
2011-2012-2013
2014-2015-2016
2017-2018-2019
2020-2021-2022
2023-2024-2025
2026-2027-2028
2029-2030-2031
2032-2033-2034
2035-2036-2037
2038-2039-2040
2041-2042-2043
2044-2045-2046
2047-2048-2049
2050-2051-2052
2053-2054-2055
2056-2057-2058
2059-2060-2061
2062-2063-2064
2065-2066-2067
2068-2069-2070
2071-2072-2073
2074-2075-2076
2077-2078-2079
2080-2081-2082
2083-2084-2085
2086-2087-2088
2089-2090-2091
2092-2093-2094
2095-2096-2097
2098-2099-2100
2101-2102-2103
2104-2105-2106
2107-2108-2109
2110-2111-2112
2113-2114-2115
2116-2117-2118
2119-2120-2121
2122-2123-2124
2125-2126-2127
2128-2129-2130
2131-2132-2133
2134-2135-2136
2137-2138-2139
2140-2141-2142
2143-2144-2145
2146-2147-2148
2149-2150-2151
2152-2153-2154
2155-2156-2157
2158-2159-2160
2161-2162-2163
2164-2165-2166
2167-2168-2169
2170-2171-2172
2173-2174-2175
2176-2177-2178
2179-2180-2181
2182-2183-2184
2185-2186-2187
2188-2189-2190
2191-2192-2193
2194-2195-2196
2197-2198-2199
2200-2201-2202
2203-2204-2205
2206-2207-2208
2209-2210-2211
2212-2213-2214
2215-2216-2217
2218-2219-2220
2221-2222-2223
2224-2225-2226
2227-2228-2229
2230-2231-2232
2233-2234-2235
2236-2237-2238
2239-2240-2241
2242-2243-2244
2245-2246-2247
2248-2249-2250
2251-2252-2253
2254-2255-2256
2257-2258-2259
2260-2261-2262
2263-2264-2265
2266-2267-2268
2269-2270-2271
2272-2273-2274
2275-2276-2277
2278-2279-2280
2281-2282-2283
2284-2285-2286
2287-2288-2289
2290-2291-2292
2293-2294-2295
2296-2297-2298
2299-2300-2301
2302-2303-2304
2305-2306-2307
2308-2309-2310
2311-2312-2313
2314-2315-2316
2317-2318-2319
2320-2321-2322
2323-2324-2325
2326-2327-2328
2329-2330-2331
2332-2333-2334
2335-2336-2337
2338-2339-2340
2341-2342-2343
2344-2345-2346
2347-2348-2349
2350-2351-2352
2353-2354-2355
2356-2357-2358
2359-2360-2361
2362-2363-2364
2365-2366-2367
2368-2369-2370
2371-2372-2373
2374-2375-2376
2377-2378-2379
2380-2381-2382
2383-2384-2385
2386-2387-2388
2389-2390-2391
2392-2393-2394
2395-2396-2397
2398-2399-2400
2401-2402-2403
2404-2405-2406
2407-2408-2409
2410-2411-2412
2413-2414-2415
2416-2417-2418
2419-2420-2421
2422-2423-2424
2425-2426-2427
2428-2429-2430
2431-2432-2433
2434-2435-2436
2437-2438-2439
2440-2441-2442
2443-2444-2445
2446-2447-2448
2449-2450-2451
2452-2453-2454
2455-2456-2457
2458-2459-2460
2461-2462-2463
2464-2465-2466
2467-2468-2469
2470-2471-2472
2473-2474-2475
2476-2477-2478
2479-2480-2481
2482-2483-2484
2485-2486-2487
2488-2489-2490
2491-2492-2493
2494-2495-2496
2497-2498-2499
2500-2501-2502
2503-2504-2505
2506-2507-2508
2509-2510-2511
2512-2513-2514
2515-2516-2517
2518-2519-2520
2521-2522-2523
2524-2525-2526
2527-2528-2529
2530-2531-2532
2533-2534-2535
2536-2537-2538
2539-2540-2541
2

TABLE OF CONTENTS

Introduction	1
Spatial Attenuation	1
Spectral Attenuation	3
Corner Frequencies and Seismic Moment	4
Discussion	5
Acknowledgements	6
References	6

LIST OF TABLES

1. Earth Model for Synthetic Lg	9
2. Earthquake Catalog Parameters	10
3. Source Parameters	11

LIST OF FIGURES

1. Distribution of ECTN Stations & Location of the Miramichi Source Zone.	12
2. Comparison of Lg Geometrical Spreading Made by Regressing Peak Amplitudes of the Synthetic Data Set With Distance Using Time Domain, Top, and Smoothed Spectral Amplitudes in the Frequency Domain, Bottom, as a Function of the Butterworth Filter Center Frequency.	13
3. Digital Data From the Station WBO for Event No. 5. The Broadband Signal is Given in the Top Trace, While the Filtered Traces are Shown Below.	14
4. Lg-Q Values Determined From Time Domain (a) and Frequency Domain (b) Analysis. 95% Confidence Limits are Given.	15
5. Lg-Q Values From Time Domain. Circles Represent Use of Data at All Distances, Asterisks the Use of Data at Distances Less than 600 km, and the Diamonds the Use of Data Corrected for the Sn Coda.	16
6. Displacement Spectral Ratio of Event No. 1 to Event No. 3 Recorded at Stations EBN (a) and LPQ (b). The Arrows Indicate the Corner Frequencies and the Solid Line an f^{-2} Trend. The Vertical Scale is in Arbitrary Units.	17

7. Example of a Semilog Plot of Acceleration Spectra at Station GNT for Events No. 3 and 5. The Solid Line Indicates the Mean Slope Corresponding to $Q=1853$ for This Station. The Slope is Determined Using Data in the 3.0 - 8.0 Hz Range. 18
8. Map Showing the Source Region, Star, and the High Frequency Q Determined for Each Station, Which is Plotted Adjacent to the Station Location. 19
9. Plot of Lg Corner Frequency, f_c , Versus Seismic Moment, M_0 , for the Events Studied. The Scaling Laws Proposed by Nuttli (1983) and Hasegawa (1983) are Shown for Comparison. 20
10. Plot of Seismic Moment, M_0 , Versus m_{Lg} . The Circles are the ECTN Catalog Values and the Asterisks are Those Determined in This Study. In Addition, the Nuttli (1983) Scaling Law for Mid-plate Earthquakes and the Hasegawa (1983) Relation for Eastern Canada are Given. 21

Lg Attenuation and Source Studies using 1982 Miramichi Data

by T.-C. Shin and R. B. Herrmann

Abstract

Using data from earthquakes in the 1982 Miramichi earthquake source zone, spectral excitation and attenuation of the Lg phase is studied. With data in the distance range of 135 to 994 km, interpretation is complicated by the presence of high frequency Sn and Pn waves which interfere with the Lg wave. At the larger distances, the signal at frequencies above 7 Hz is completely dominated by the non-Lg arrivals. A frequency dependent Lg-Q is determined which rises from 300 at 0.5 Hz to about 1400 at 10 Hz at which it flattens at higher frequency. The Sn coda apparent Q rises above 3000 at frequencies higher than 10 Hz. Seismic moment and corner frequency estimates are made using Lg-Q corrected spectra. The moment estimates compare well with those obtained from long period surface waves and short distance spectral estimates. The Lg corner frequency estimates are substantially lower than the short distance estimates. This discrepancy is the subject of discussion, but the Lg moment-corner frequency estimates do model observed data well when using a Brune (1970) source model and the derived attenuation relation.

INTRODUCTION

The 1982 sequence of earthquakes near Miramichi, New Brunswick has been the subject of many studies (Choy *et al.*, 1983; Cranswick *et al.*, 1982; Mueller and Cranswick, 1985; Saikia and Herrmann, 1985; Wetmiller *et al.*, 1984) which discuss earthquake locations, focal mechanism and source dynamics based on teleseismic and local observations. Regional data are also available from stations of the Eastern Canada Telemetered Network (ECTN) at distances of 135 to 994 km from the focal region.

The ECTN is a digitally telemetered network consisting of vertical component instruments with a system velocity sensitivity that is essentially flat between corner frequencies of 1.0 and 16.0 Hz (Hasegawa, 1985). Data from the ECTN have previously been used to estimate seismic moments and corner frequencies of eastern Canada earthquakes (Hasegawa, 1983) and to study Lg-wave attenuation (Hasegawa, 1985). Hasegawa (1985) used earthquakes with travel paths to ECTN stations that were within or along the edge of the Canadian shield. Data paths for sources in the east in the structurally complex Appalachian province were excluded from his study. The purpose of this present study is to use ECTN data to examine the Lg-wave attenuation for those paths excluded by Hasegawa (1985) and then to compare results.

SPATIAL ATTENUATION

Figure 1 is a map of eastern Canada showing the location of the Miramichi source region and the sites of the ECTN stations used in the study. The ECTN data are acquired at 60 samples a second. Since this study is interested in the frequency dependent excitation and attenuation of the Lg signal, the observed signals are filtered through fifteen different Butterworth bandpass filters whose high- and low-frequency responses fall and rise, respectively, at 24 db/octave. The filter center frequencies were in the range from 0.5 to 15.0 Hz and the filter bandwidth was taken to be 0.7 times the center frequency.

The Lg spatial data are fit by a model of the form

$$A(r) = A_0 r^{-n} e^{-\gamma} \quad (1)$$

where n is a coefficient that is taken to be $n = 5/6$ for Lg time domain measurements and $n = 1/2$ for frequency domain measurements. The parameter γ is related to Q by

$$\gamma = \frac{\pi f}{QU} \quad (2)$$

where f is the frequency and U is the group velocity of the wave propagation, taken to be 3.5

km/sec.

To process the data, different approaches were used for time and frequency domain measurements. The time domain study is performed by applying a recursive digital Butterworth filter to the data, and peak amplitudes are read in the time window corresponding to the Lg arrival. To make frequency domain measurements, a 17.07 second time window, corresponding to 1024 time domain samples, is used about the expected Lg arrival. The signal is Fourier transformed, the instrument response removed, and the amplitude spectra at the desired center frequency is obtained by averaging the amplitude spectra between the two corner frequencies of filter.

To test the methodology for interpretation, we synthesized the vertical component Lg-wave at each seismograph station by adding up all higher mode surface waves for the earth model of Table 1. A source depth of 5 km, a focal mechanism with 60° dip, 100° slip and 200° strike were assumed. Synthetic seismograms were generated at a sampling interval of 60 samples per second. Three sets of synthetics were generated corresponding to source corner frequencies of 1, 2 and 3 Hz. The signals included the ECTN instrument response in order to make the synthetics comparable to the actual observed ECTN data. The same processing steps are then applied to the data sets. Approximately 700 seconds of time history were synthesized at each station.

The first test was to measure the peak Lg amplitude as a function of distance for each earthquake using the synthetics generated for a perfectly elastic model. Equation (1) is then used with $\gamma = 0$ to determine the coefficient n . This exercise led to an $n = 0.834$, which is in agreement with previous assumptions (Nuttli, 1973) about the spatial decay of the broad band Lg wave. The next step involved the use of the bandpass filtered signals. Figure 2 presents the geometrical spreading factors n obtained from the smoothed spectral estimates and the filtered time domain signals. The solid horizontal lines indicate the values of $n = 5/6$ for the time domain and $n = 1/2$ for the frequency domain studies. The errors arise from the fact that Lg wave amplitudes do not vary in a uniform manner with distance and because radiation pattern effects for the focal mechanism used can cause azimuthal amplitude variation not accounted for by the model. From this exercise, we conclude that the bandpass filters used are not really so narrow that time domain geometrical spreading cannot be used for the recursively filtered data. This is really expected from surface wave theory because the additional time domain decay is really due to the increasing duration of the signal with distance, and this will also be apparent in the signals filtered as described here.

The geometrical spreading of the filtered time domain data is not exactly the $n = 5/6$ expected for time domain data. However, considering the error bars, we will use the $n = 5/6$ for the filtered time domain signal. If the actual geometrical spreading is somewhat less, this will mean that the inferred γ value is somewhat low and the corresponding Q value somewhat high.

Table 2 gives the epicentral coordinates, identification code, and ECTN published magnitude for each event studied. The range of data covers over three units in short period magnitude, making the data set an excellent one for analysis.

Prior to performing any detailed analysis it is essential that the data be examined. Data at short distances were as expected, with the Lg arrival being the largest signal in all frequency bands. However, we observed an interesting phenomena at distances greater than 500 km. Figure 3 illustrates an this feature of the data for the recording of event No. 5 at the station WBO, an epicentral distance of 702 km from the source. The top trace gives the broadband data, while the other traces are narrow band pass filtered at the indicated center frequencies. The peak Lg arrival is indicated by the arrow at the top of the figure. The Lg arrival is distinct at the low frequencies, but quickly disappears within the mantle Sn coda, which is itself riding on top of the mantle Pn coda. The implication of this observation, is that we can not arbitrarily window the trace about the Lg arrival and expect the spectrum to tell us everything about the Lg at all frequencies. With this particular signal, we can only use frequency up to 7.0 Hz if we are able to determine how much the Lg rises above the coda of the Sn.

Equation (1) is easily linearized and adapted to multiple events. The regression analysis yields a single value of γ , which is related to Q by (2), and an A_0 term for each event proportional

to the source excitation at each filter center frequency. The inferred Q values from the time domain and frequency domain measurements using *all data at all distances* are shown in Figure 7. The Q estimates made in each domain agree with each other. The dependence of Lg - Q with frequency can be approximately modeled by the relation $Q(f) = (500-550)f^{0.66}$. An examination of the data indicates a distinct change in the frequency dependence of Q at about 7 Hz. Above this frequency there is a definite linear trend, while below this frequency there is a suggestion that the Lg Q is attempting to flatten at higher frequencies.

Because of the observation that the Lg arrival time window is contaminated by the Sn and Pn coda at higher frequencies and large distances, the Q values given above are suspect above 7 Hz. To resolve this mixture of time domain data types, two approaches were taken. The first used the data at all distances for frequencies less than 7 Hz, and data acquired at distances less than 600 km for the higher frequencies. These Q values are shown as the squares for low frequencies and as the asterisks at higher frequencies in Figure 5. The circles in Figure 5 are the time domain results shown in Figure 4a. The asterisks have large 95% confidence limits because of the reduced distance coverage. The asterisks support the flattening of $Q(f)$ at higher frequency suggested by the low frequency data.

The second approach attempts to use the Lg data at larger distances by estimating the Lg amplitude. To do this we consider the envelope of the Lg arrival to be sitting upon a predictable envelope of the Sn arrival and its coda. We fit the Sn coda shape using an Aki and Chouet (1975) body-wave scattering model. Subtracting the estimated coda envelope from the observed envelope permits an estimate of the peak Lg amplitude. The modified data set is used in the regression analysis to yield the Q estimates given by the diamonds in Figure 5. This approach yields Q values at higher frequencies intermediate between the other two estimates.

SPECTRAL ATTENUATION

Anderson and Hough (1984) presented an interesting discussion of modeling the high frequency falloff of acceleration spectra in which they showed that a linear trend was observable if a semi-logarithmic plot of acceleration spectra as a function of frequency is made. This linear trend indicates that at high frequencies the acceleration spectra can be modeled by an exponential decay operator. They further found that the exponential decay increased with distance which could be explained by a distance independent site effect and a distance dependent propagation effect.

The acceleration spectra $A(f)$ can be parametrically described by combining a Brune (1970) source spectrum and an attenuation operator as

$$A(f) = \frac{A_0}{1 + (f_c/f)^2} e^{-\pi f t / Q} \quad (3)$$

where f_c is the corner frequency, t is the travel time of the arrival, and Q is the apparent propagation Q . If the model is correct, then a semi-logarithmic plot of $A(f)$ vs f will exhibit a linear trend at frequencies greater than the corner frequency. If the model is incorrect, the data may exhibit an apparent linear trend if only a narrow range of frequencies is considered. One way to test the appropriateness of the Brune (1970) model is to form the spectral ratio of two events at the same distance. The common attenuation effect divides out, and the resulting ratio will exhibit a f^{-2} trend between the corner frequencies if the event with the higher corner frequency has a lower displacement spectral level at high frequencies, which is usually the case. The f^{-2} trend is a direct consequence of the model. Figure 6 compares the displacement spectral ratios of events 1 to 3 at EBN, 135 km, and LPQ, 257 km, from the source zone. The solid line indicates an f^{-2} trend and the arrows indicate the corner frequencies estimated by fitting the A_0 source terms of the regression analysis to a Brune (1970) spectrum. The vertical axis is plotted in arbitrary units and no correction has been made for noise. The noise level for the smaller earthquake is equivalent to the signal level at frequencies less than 0.5 Hz. This exercise indicates that the omega-squared spectral model is reasonable, although the plots are not overwhelmingly convincing.

Figure 7 shows the results of processing the acceleration spectra of events 3 and 5 at the

station GNT. The straight line indicates the inferred linear trend. Based on the appearance of the linear trends, weights were assigned to each slope determination as were windows between which the slopes were to be determined. In this figure, data were used in the 3 - 8 Hz range, and the slope was determined to be $-0.0930 \log_{10}$ units per Hz. If we assume a group velocity of 3.5 km/s to the station, the inferred Q is 1853 using data from 6 events. Figure 8 presents the spectral Q values determined from data at each station. The form of presentation points out the spectral Q determined seems to be very stable for a wide range of epicentral distance. Note that the Q values given here are not directly related to the spatial Q values given in Figures 4 and 5 since a single frequency independent Q value is used to model the spectra. Since this Q is based on the slope which is in turn dependent upon the high frequency spectral level, the spectral Q determined from the slope is more an indication of the high frequency Q rather than a lower frequency Q . We note that the spectral constant Q of about 1900 is within the range of possible Q values near 10 Hz in Figure 5.

CORNER FREQUENCIES AND SEISMIC MOMENT

The ground vertical component Lg-wave displacement spectra, $D(f)$, determined by correcting the observed spectra by the displacement sensitivity of the instrument, at a distance r , is modeled by a relation

$$D(f) = \frac{M_0}{4\pi\rho\beta^3} \frac{S(f)}{r_0} \left(\frac{r_0}{r}\right)^{1/2} e^{-\pi f/Q} \quad (5)$$

where M_0 is the seismic moment, ρ is the density, β is the crustal shear wave velocity, r_0 is the distance marking a change in signal character from a single body-wave arrival to surface-wave arrivals beyond this point, and $S(f)$ is a normalized Brune displacement source spectrum, given by

$$S(f) = (1 + (f/f_c)^2)^{-1}$$

This relation was given by Herrmann and Kijko (1983a) to predict the log-mean spectral level. We use the Hasegawa (1983) values of $r_0 = 100$ km, $\rho = 2.8$ gm/cm³, and $\beta = 3.8$ km/sec, to apply this relation to eastern Canada. Since we can take $Q(f) = 550f^{0.85}$, approximately, a non-linear inversion technique can be used to use (5) to determine M_0 and f_c . Table 3 presents these estimates of these parameters using all available data. The table entries give the event number, the catalog magnitude, M_N , the average f_c and its standard deviation, the log-mean estimate of the seismic moment, obtained by averaging the log moments and then taking the antilog, and the multiplicative confidence factor EM_0 to which the moments are known. The last column, N_s , gives the number of spectra used in the estimation.

In addition to listing the parameters f_c and M_0 which describe the observed data, estimates of source radius, r_0 and stress drop, $\Delta\sigma$, are given using the Brune (1970) relations

$$r_0 = \frac{2.34\beta}{2\pi f_c}$$

and

$$\Delta\sigma = \frac{7M_0}{16r_0^3}$$

We also derived an m_{Lg} magnitude by low pass filtering the ECTN trace to simulate a seismometer-galvanometer system with a 1.0 Hz seismometer and a galvanometer with 0.8 critical damping and a 1.5 Hz natural frequency. In order to truly model a WWSSN short period system, another lowpass filter at 3.0 Hz would be required to model the effect of the Benioff seismometer inductance, the equivalent response of the simulated seismograms is sufficiently similar to that of the WWSSN short period instrument to be used in determining the m_{Lg} magnitude. We use the m_{Lg} definition of Herrmann and Nuttli (1982)

$$m_{Lg}(f) = 2.94 + 0.833 \log_{10}(r/10) + 0.4342 \gamma r + \log_{10} A(r, f). \quad (6)$$

where r is the epicentral distance in km, A is the reduced ground amplitude in microns at

frequency f , and γ is the regional spatial Lg attenuation coefficient and here equals 0.00183 km^{-1} at 1.5 Hz. Herrmann and Kijko (1983b) showed that this relation can be used with instruments other than the WWSSN short period if used as described. The values of the computed m_{Lg} are also given in Table 3, and can be compared to the ECTN catalog values. The computed m_{Lg} values have standard deviations varying between 0.16 and 0.22 magnitude units.

An independent check of the derived seismic moments was made by comparing the source terms determined from the regression of the frequency domain Lg spectra against distance. There was good agreement. We also corrected each spectra for $Q(f)$, equalized for surface wave geometrical spreading, and determined an RMS average amplitude spectrum. These agreed very well with the spectra predicted for the source parameters of Table 3.

Figure 9 compares the seismic moment - corner frequency values determined in this study with a scaling law proposed by Nuttli (1983) and with observed scaling on the Canadian Shield that Hasegawa (1983) obtained using ECTN data. Figure 10 plots the seismic moment versus magnitude values. The circles use the ECTN catalog magnitudes and the asterisks use the m_{Lg} values determined in this study. The Nuttli (1983) proposed scaling law and the empirical Hasegawa (1983) scaling laws are shown for reference.

DISCUSSION

This paper has presented a number of source parameter and attenuation estimates that must be evaluated in light of other studies. The seismic moment estimates are quite acceptable. Nguyen (1985) determined a seismic moment of 5.9×10^{23} dyne-cm for event 1 by performing a simultaneous inversion for focal mechanism, focal depth and seismic moment from long period Love- and Rayleigh-wave data recorded in North America. This agrees well with our Lg estimate of 5.6×10^{23} dyne-cm. Saikia and Herrmann (1985) modeled three component time history data from data within 10 km of the source of event 3, and estimated the seismic moment to be in the range of $3.3 - 4.1 \times 10^{20}$ dyne-cm, to which our estimate 5.9×10^{20} dyne-cm agrees well. Some of the events of this study also provided locally recorded data analyzed by Mueller and Cranswick (1985). These were events 3, 11, 12, 13 14, 15 and 16. Mueller and Cranswick (1985) used spectral techniques to estimate the seismic moments, corner frequencies and stress drops. Keeping in mind that our seismic moments for events 11 through 16 were based on only one vertical component spectra, the agreement of the estimates is quite good. Our estimates are usually less than a factor of 2 greater than theirs, the only exception being event 15 for which our moment is approximately 2.5 to 3 times greater than theirs. This comparison of Lg seismic moment estimates with other independent estimates points out the stability of Lg seismic moment estimates when care is taken to account for anelastic attenuation.

The value of using Lg-wave corner frequency estimates to infer source properties is currently the subject of considerable discussion (Mueller and Cranswick, 1985). There seems to be an apparent contradiction in that the Lg inferred stress drops are usually lower than the comparable estimates using short distance data. We would like to avoid this issue for the present by stating that the combination of a Brune (1970) source spectrum model and an attenuation operator successfully fit *all* observed spectra (Appendix B, Shin, 1985). Using short distance data for event 3, Mueller and Cranswick (1985) found S-wave corner frequencies in the range of 6 - 15 Hz, while Saikia and Herrmann (1985) found values in the range of 15 - 20 Hz for the same data set. The Lg-corner frequency of Table 3 is constrained to be near 3.5 Hz. One major difference in the data sets is that the short distance spectra could not be fit by a Brune (1970) omega-squared spectrum, but rather required high frequency displacement spectrum falloff with frequency greater than f^{-2} , sometimes greater than f^{-6} ! To further complicate the comparison of short distance spectral estimates to large distance Lg spectral estimates, Cranswick *et al* (1985) discussed the problems with near surface site resonances, which can either increase or decrease the apparent corner frequency depending upon the resonance frequency. One can argue that the Lg may be the more robust indicator of source properties since it samples more of the focal sphere, it has different angles of incidence at the receiver which may smooth out the resonance effects seen in a single incident ray, and by the fact that its randomness of arrivals avoids the coherence required for resonance. The Lg study does support a higher frequency content in the source than does the Nuttli (1983) scaling

model, as seen in Figure 9.

The attenuation estimates are not without some ambiguity either. We have found that it is difficult to see the Lg wave at high frequencies at large distances for these travel paths crossing into the Canadian Shield because it attenuates faster than the coda following the Sn and Pn (Figure 3). This observation complicates the analysis of Lg-Q but also indicates that high frequency waves can propagate large distances in the upper mantle. This observation is only now being made because of seismographs recording in this frequency range. Our estimate of Lg-Q for the region is given in Figure 5. Until further data are analyzed at high frequency, our preferred model would be to have the Lg-Q rise sharply at low frequencies and then flatten to about 1500-2000 at high frequencies. This would explain the Lg spectral Q of 1800 or so observed at short distances, and would also admit the possibility of the Sn coda overwhelming the Lg at larger distances. The mantle Sn and its coda can be presumed to be a problem only beyond the distance at which Sn first appears. Hasegawa (1985) modeled vertical component acceleration data derived from the ECTN recordings and concluded that the Lg-Q was $Q(f) = 900f^{0.2}$. This estimate, based on a larger data set, but a different set of propagation paths, is within the error bars of our estimates at frequencies greater than 2.0 Hz. The Hasegawa (1985) has better statistical properties because of the wider range of epicentral distances available, whereas this study used 16 earthquakes recorded at 16 stations, with the source receiver distances fixed.

The seismograms we examined indicated a relationship between arrivals expected from wave theory and those due to a scattering mechanism. Following Dainty (1981) the frequency dependence of the observed Lg-Q, $Q_{obs}(f)$, can be expressed as

$$Q_{obs}(f)^{-1} = Q_{abs}^{-1} + (Q_{0,scat}f)^{-1}$$

which states that the observed $Q(f)$ is a superposition of a frequency independent intrinsic, absorptive Q, and a frequency dependent scattering Q. For our data set we would estimate the intrinsic Q to be about 1500-2000 and the Q_0 to be about 600.

ACKNOWLEDGMENTS

The authors wish to thank the Earth Physics Branch, Energy Mines and Resources Canada for providing the excellent digital data used in the study. The special assistance of H. Hasegawa is very much appreciated. The work discussed was done in fulfillment of the Ph. D. degree by the senior author. This work was supported by the U. S. Nuclear Regulatory Commission under Contract NRC-04-81-195-03, by the U. S. Geological Survey under Contract 14-08-0001-21999, and by NSF Grant CEE-8406577.

REFERENCES

- Aki, K. and B. Chouet (1975). Origin of coda waves: source, attenuation, and scattering effects, *J. Geophys. Res.* **80**, 3322-3342.
- Anderson, J. G. and S. E. Hough (1984). A model for the shape of the Fourier amplitude spectrum of acceleration at high frequencies, *Bull. Seism. Soc. Am.* **74**, 1969-1995.
- Brune, J. N. (1970). Tectonic stress and the spectra of seismic shear waves from earthquakes, *J. Geophys. Res.* **75**, 4997-5009.
- Choy, G. L., J. Boatwright, J. W. Dewey, and S. A. Sipkin (1983). A teleseismic analysis of the New Brunswick earthquake of January 9, 1982, *J. Geophys. Res.* **88**, 2199-2212.
- Cranswick, E., C. Mueller, R. Wetmiller, and E. Senbera (1982). Local multi-station digital recordings of aftershocks of the January 9, 1982 New Brunswick earthquake, *U. S. Geol. Surv., Open-File Rept.* 82-777.
- Cranswick, E., R. Wetmiller, and J. Boatwright (1985). High-frequency observations and source parameters of microearthquakes recorded at hard-rock sites, *Bull. Seism. Soc. Am.* **75**,

1535-1567.

- Dainty, A. (1981). A scattering model to explain seismic Q observations in the lithosphere between 1 and 20 Hz, *Geophys. Res. Letters* **11**, 1126-1128.
- Hasegawa, H. S. (1983). Lg spectra of local earthquakes recorded by the Eastern Canada Telemetered Network and spectral analysis, *Bull. Seism. Soc. Am.* **73**, 1041-1062.
- Hasegawa, H. S. (1985). Attenuation of Lg waves in the Canadian shield, *Bull. Seism. Soc. Am.* **75**, 1569-1582.
- Herrmann, R. B. and O. W. Nuttli (1982). Magnitude: The relation of M_L to m_{bLg} , *Bull. Seism. Soc. Am.* **72**, 389-399.
- Herrmann, R. B. and A. Kijko (1983a). Modeling some empirical Lg relations, *Bull. Seism. Soc. Am.* **73**, 157-162.
- Herrmann, R. B. and A. Kijko (1983b). Short-period Lg magnitudes: instrument, attenuation and source effects, *Bull. Seism. Soc. Am.* **73**, 1835-1850. Mueller, C. S. and E. Cranswick (1985). Source parameters from locally recorded aftershocks of the 9 January 1982 Miramichi, New Brunswick earthquake, *Bull. Seism. Soc. Am.* **75**, 337-360.
- Nguyen, B. V. (1985). Surface-wave focal mechanisms, magnitudes, and energies for some earthquakes in eastern North America with tectonic implication, *M. S. Thesis*, Saint Louis University, Saint Louis, Missouri.
- Nuttli, O. W. (1983). Average seismic source parameter relation for mid-plate earthquakes, *Bull. Seism. Soc. Am.* **73**, 519-536.
- Saikia, C. K. and R. B. Herrmann (1985). Application of waveform modeling to determine focal mechanisms of four 1982 Miramichi aftershocks, *Bull. Seism. Soc. Am.* **75**, 1021-1040.
- Shin, T.-C. (1985). Lg and Coda Wave Studies of Eastern Canada, *Ph. D. Dissertation*, Saint Louis University, Saint Louis, Missouri (available through University Microfilms, Ann Arbor, Michigan).
- Wetmiller, R. J., J. Adams, F. M. Anglin, H. S. Hasegawa, and A. E. Stevens (1984). Aftershock sequences of the 1982 Miramichi, New Brunswick, earthquake, *Bull. Seism. Soc. Am.* **74**, 621-654.

Department of Earth and Atmospheric Sciences
Saint Louis University
P. O. Box 8099
St. Louis, Missouri 63156

Figure Captions

- Fig. 1. Distribution of ECTN stations and location of the Miramichi source zone (star).
- Fig. 2. Comparison of Lg geometrical spreading made by regressing peak amplitudes of the synthetic data set with distance using time domain, top, and smoothed spectral amplitudes in the frequency domain, bottom, as a function of the Butterworth filter center frequency.
- Fig. 3. Digital data from the station WBO for event No. 5. The broadband signal is given in the top trace, while the filtered traces are shown below.
- Fig. 4. Lg-Q values determined from time domain (a) and frequency domain (b) analysis. 95 % confidence limits are given.
- Fig. 5. Lg-Q values from time domain. Circles represent use of data at all distances, asterisks the use of data at distances less than 600 km, and the diamonds the use of data corrected for the Sn coda.
- Fig. 6. Displacement spectral ratio of event No. 1 to event No. 3 recorded at stations EBN (a) and LPQ (b). The arrows indicate the corner frequencies and the solid line an f^{-2} trend. The vertical scale is in arbitrary units.
- Fig. 7. Example of a semilog plot of acceleration spectra at station GNT for events No. 3 and 5. The solid line indicates the mean slope corresponding to $Q=1853$ for this station. The slope is determined using data in the 3.0 - 8.0 Hz range.
- Fig. 8. Map showing the source region, star, and the high frequency Q determined for each station, which is plotted adjacent to the station location.
- Fig. 9. Plot of Lg corner frequency, f_c , versus seismic moment, M_0 , for the events studied. The scaling laws proposed by Nuttli (1983) and Hasegawa (1983) are shown for comparison.
- Fig. 10. Plot of seismic moment, M_0 , versus m_{Lg} . The circles are the ECTN catalog values and the asterisks are those determined in this study. In addition the Nuttli (1983) scaling law for mid-plate earthquakes and the Hasegawa (1983) relation for eastern Canada are given.

Table 1
Earth Model for Synthetic Lg

d(km)	α (km/sec)	β (km/sec)	ρ (gm/cc)
1	5.00	2.89	2.5
9	6.10	3.52	2.7
10	6.40	3.70	2.9
20	6.70	3.87	3.0
	8.15	4.70	3.4

Table 2
Earthquake Catalog Parameters

No.	Date	Origin time UT	Latitude N°	Longitude W°	M _N
1	11 Jan. 82	21:41:08	46.6	66.6	5.40
3	17 Jan. 82	13:33:56	46.6	66.6	3.50
5	31 Mar. 82	21:02:20	46.6	66.6	5.10
6	04 Apr. 82	13:50:12	46.6	66.6	4.30
7	11 Apr. 82	18:00:53	46.6	66.6	4.00
8	18 Apr. 82	22:47:21	46.6	66.6	4.00
9	06 May 82	16:41:07	46.6	66.6	4.00
10	16 Jan. 82	15:31:22	46.6	66.6	2.06
11	16 Jan. 82	15:53:39	46.6	66.6	3.07
12	17 Jan. 82	14:08:14	46.6	66.6	2.46
13	17 Jan. 82	17:57:40	46.6	66.6	2.08
14	18 Jan. 82	02:58:46	46.6	66.6	2.16
15	19 Jan. 82	11:58:49	46.6	66.6	2.46
16	20 Jan. 82	08:21:38	46.6	66.6	2.16

M_N : Lg magnitude used in ECTN

Table 3
SOURCE PARAMETERS

No.	M_N	m_{Lg}	f_c Hz	Ef_c Hz	M_o dyne-cm ($\times 10^{22}$)	EM_o	r_o km	$\Delta\sigma$ bars	N_S
1	5.40	5.73	0.51	0.11	55.80	1.95	2.758	11.646	13
3	3.50	3.74	3.44	0.06	0.059	2.57	0.411	3.719	9
5	5.10	5.00	0.85	0.14	11.17	2.51	1.651	10.857	14
6	4.30	4.47	2.33	0.15	0.49	2.45	0.613	9.327	10
7	4.00	4.24	2.50	0.18	0.17	2.18	0.564	4.003	11
8	4.00	4.23	2.44	0.15	0.18	2.09	0.573	4.127	12
9	4.00	4.18	2.50	0.17	0.18	2.51	0.565	4.571	10
10	2.10		10.20		0.0018		0.136	3.225	1
11	3.00		6.00		0.011		0.236	3.406	1
12	2.46		9.40		0.002		0.151	2.610	1
13	2.16		10.60		0.0014		0.134	2.496	1
14	2.08		10.80		0.0013		0.131	2.465	1
15	2.46		8.60		0.0031		0.165	3.069	1
16	2.16		10.00		0.0011		0.129	2.275	1

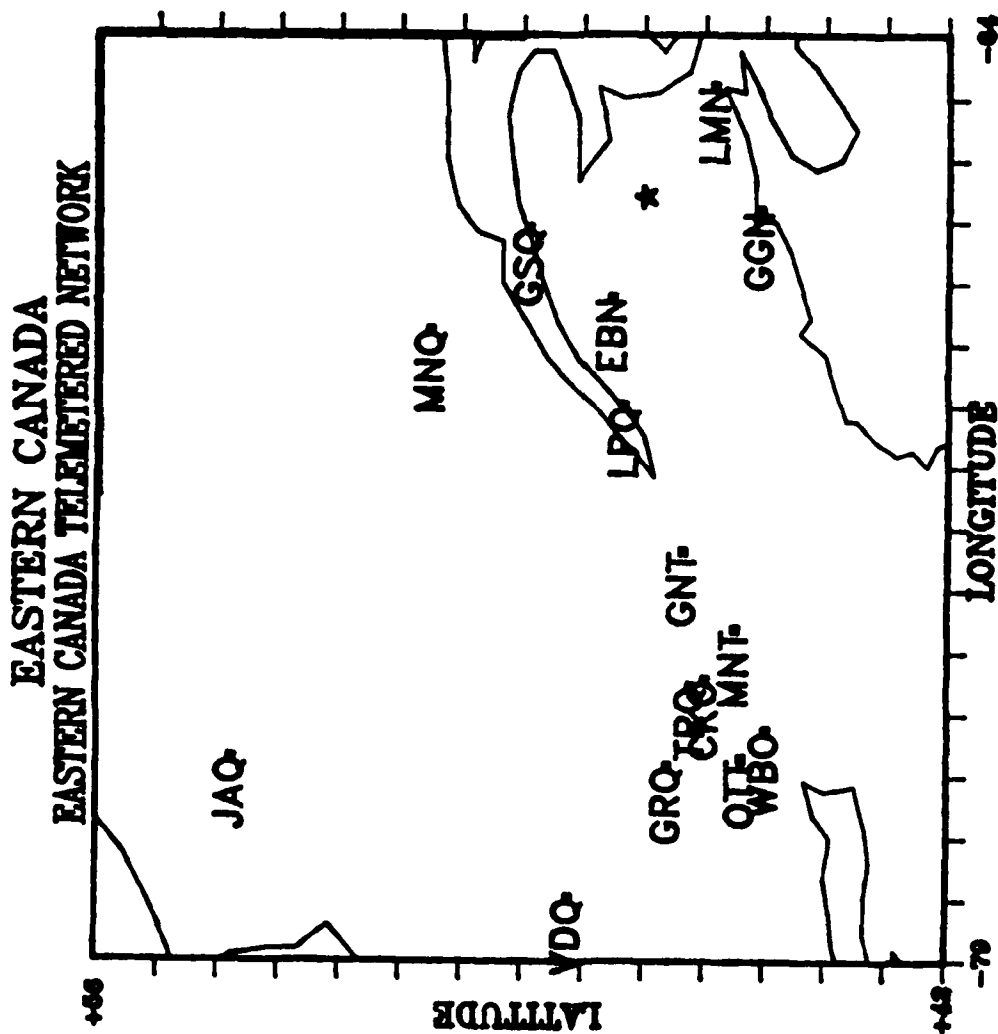


Fig. 1. Distribution of ECTN stations and location of the Miramichi source zone (star).

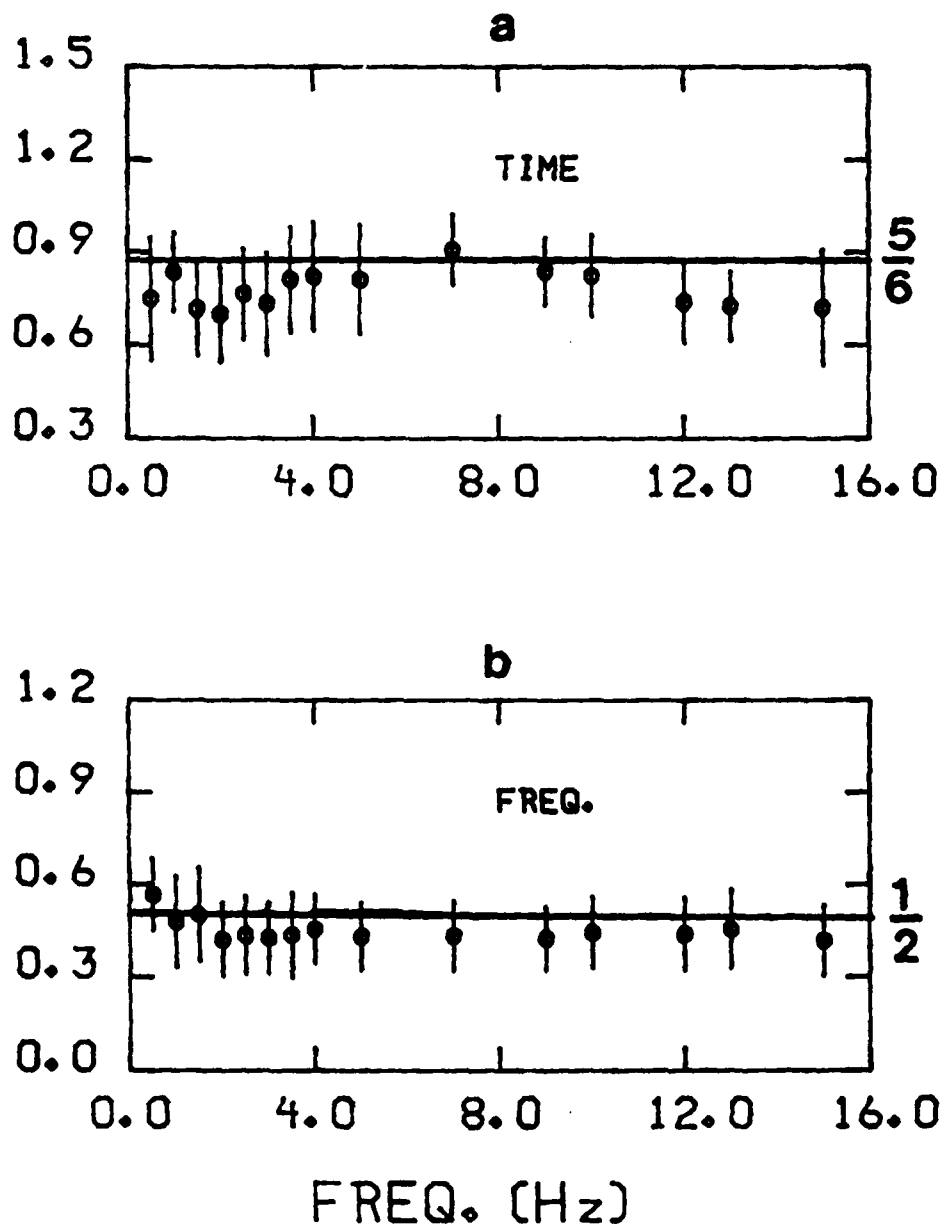


Fig. 2. Comparison of Lg geometrical spreading made by regressing peak amplitudes of the synthetic data set with distance using time domain, top, and smoothed spectral amplitudes in the frequency domain, bottom, as a function of the Butterworth filter center frequency.

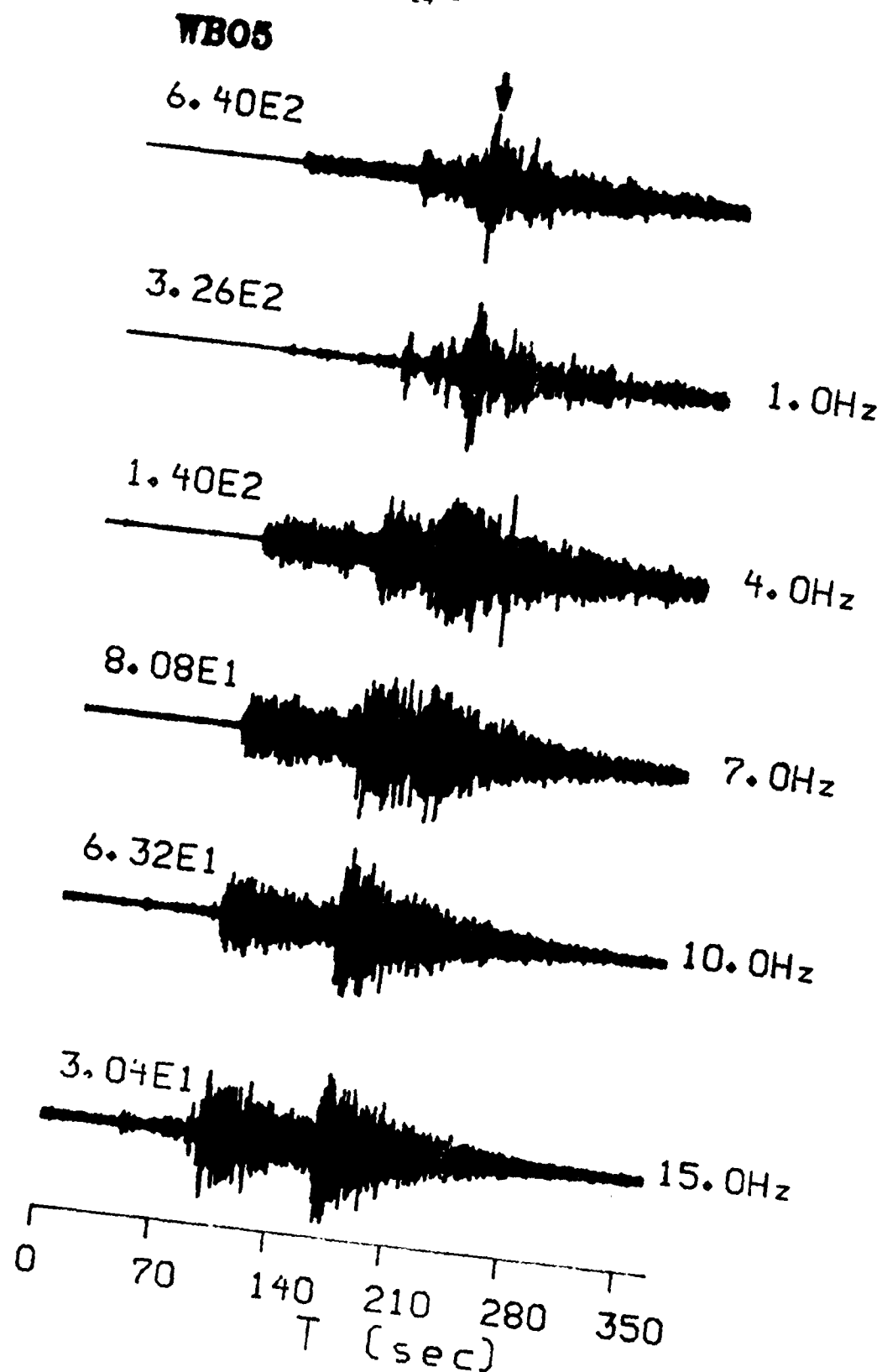


Fig. 3. Digital data from the station WBO for event No. 5. The broadband signal is given in the top trace, while the filtered traces are shown below.

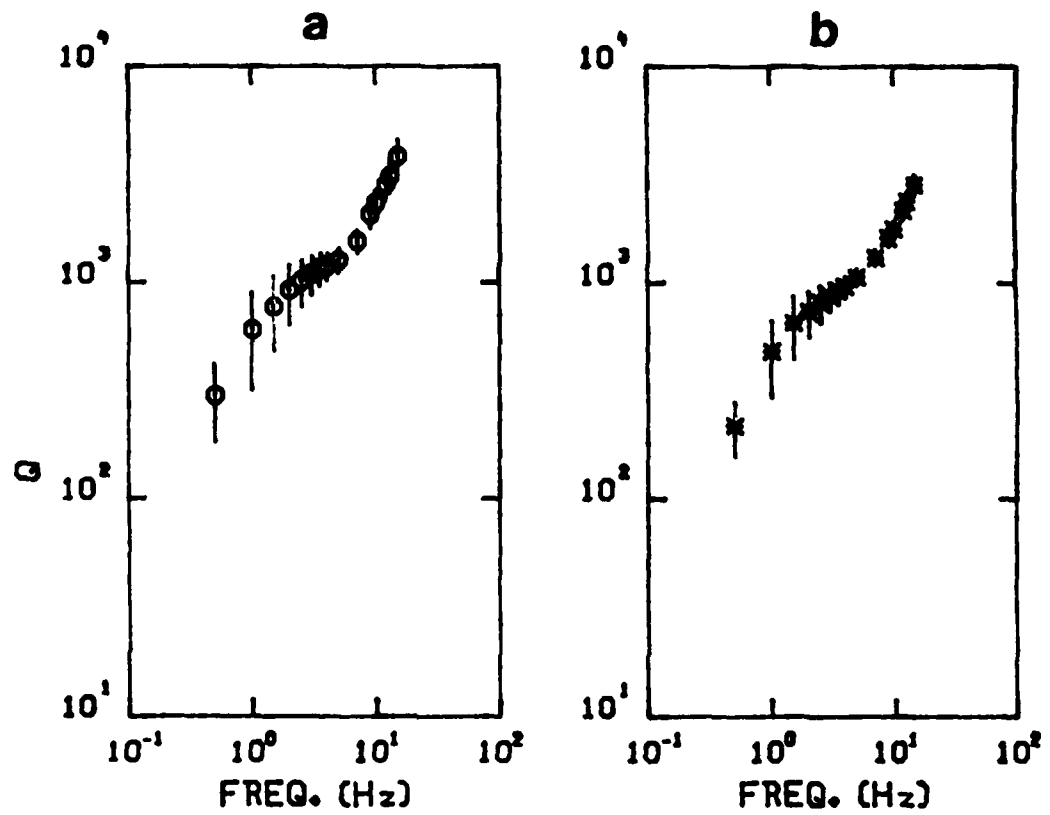


Fig. 4. Lg-Q values determined from time domain (a) and frequency domain (b) analysis. 95 % confidence limits are given.

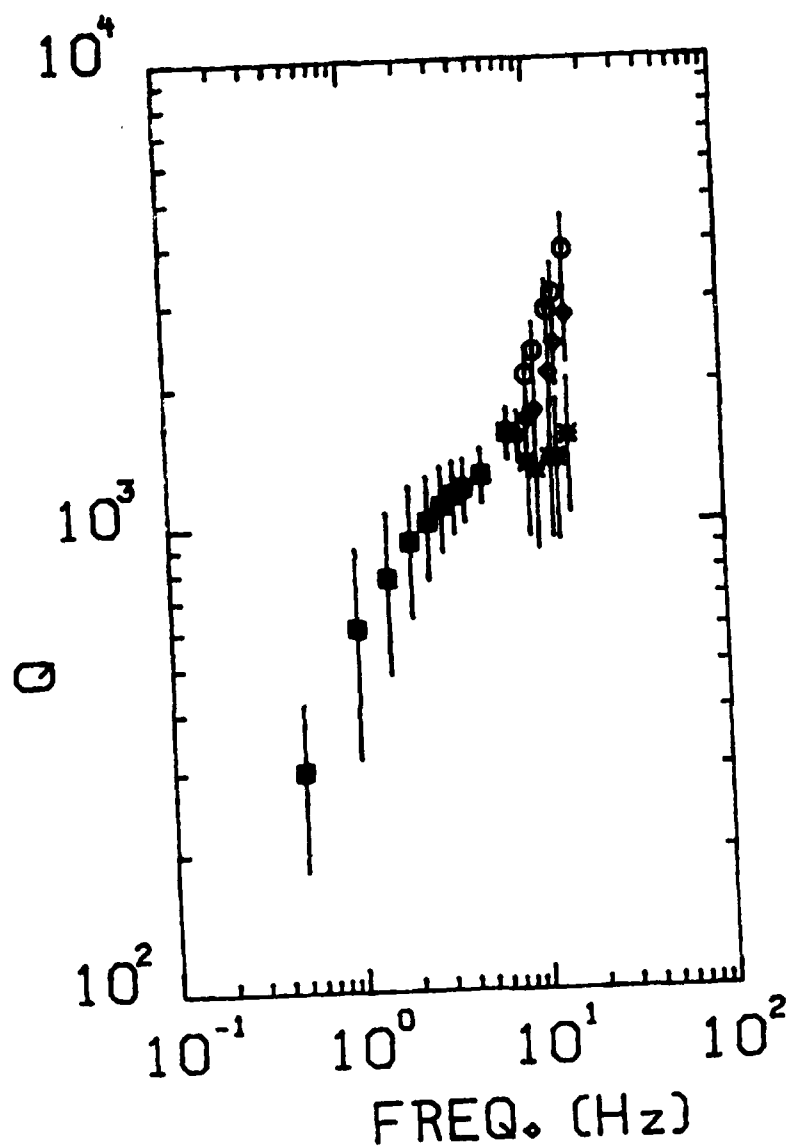


Fig. 5. Lg-Q values from time domain. Circles represent use of data at all distances, asterisks the use of data at distances less than 600 km, and the diamonds the use of data corrected for the Sn coda.

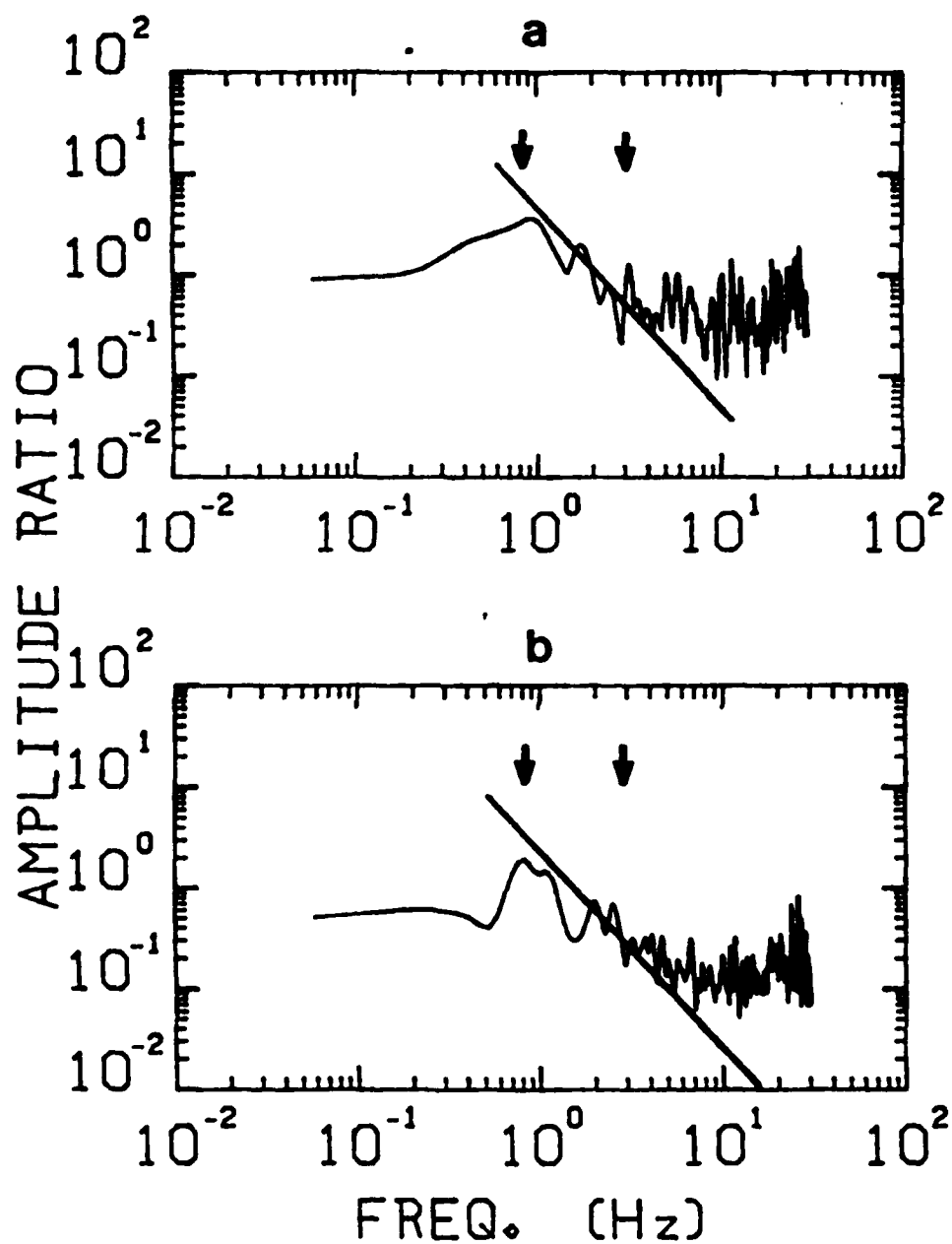


Fig. 6. Displacement spectral ratio of event No. 1 to event No. 3 recorded at stations EBN (a) and LPQ (b). The arrows indicate the corner frequencies and the solid line an f^{-2} trend. The vertical scale is in arbitrary units.

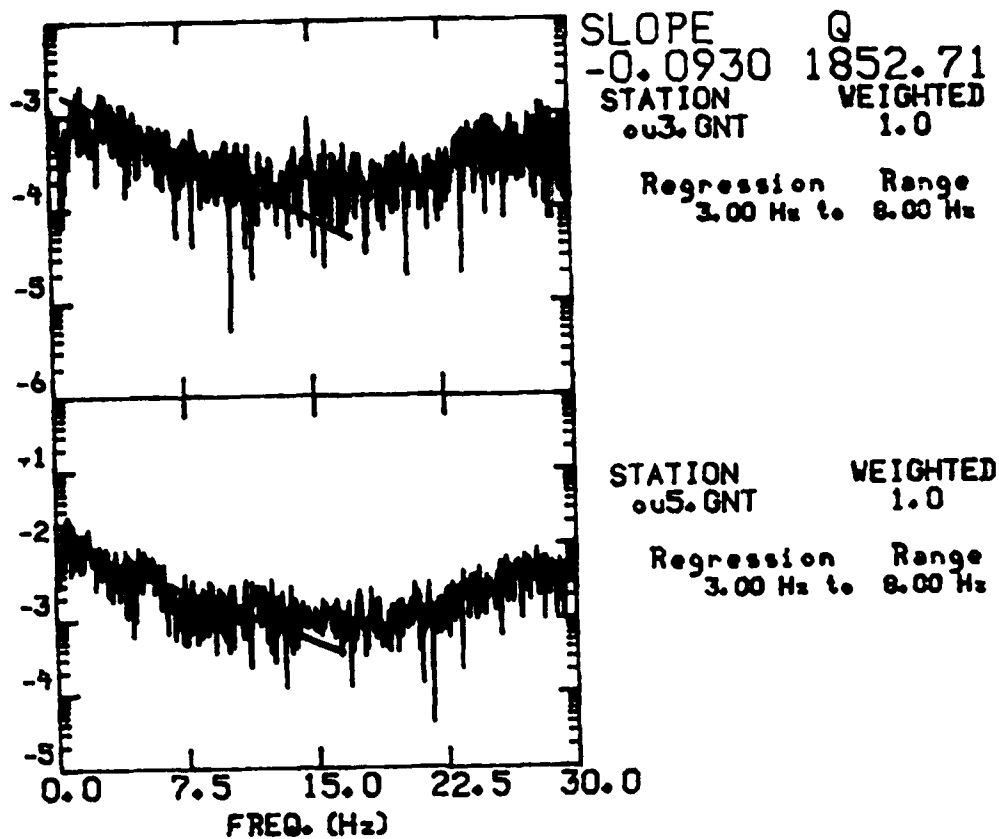


Fig. 7. Example of a semilog plot of acceleration spectra at station GNT for events No. 3 and 5. The solid line indicates the mean slope corresponding to $Q=1853$ for this station. The slope is determined using data in the 3.0 - 8.0 Hz range.

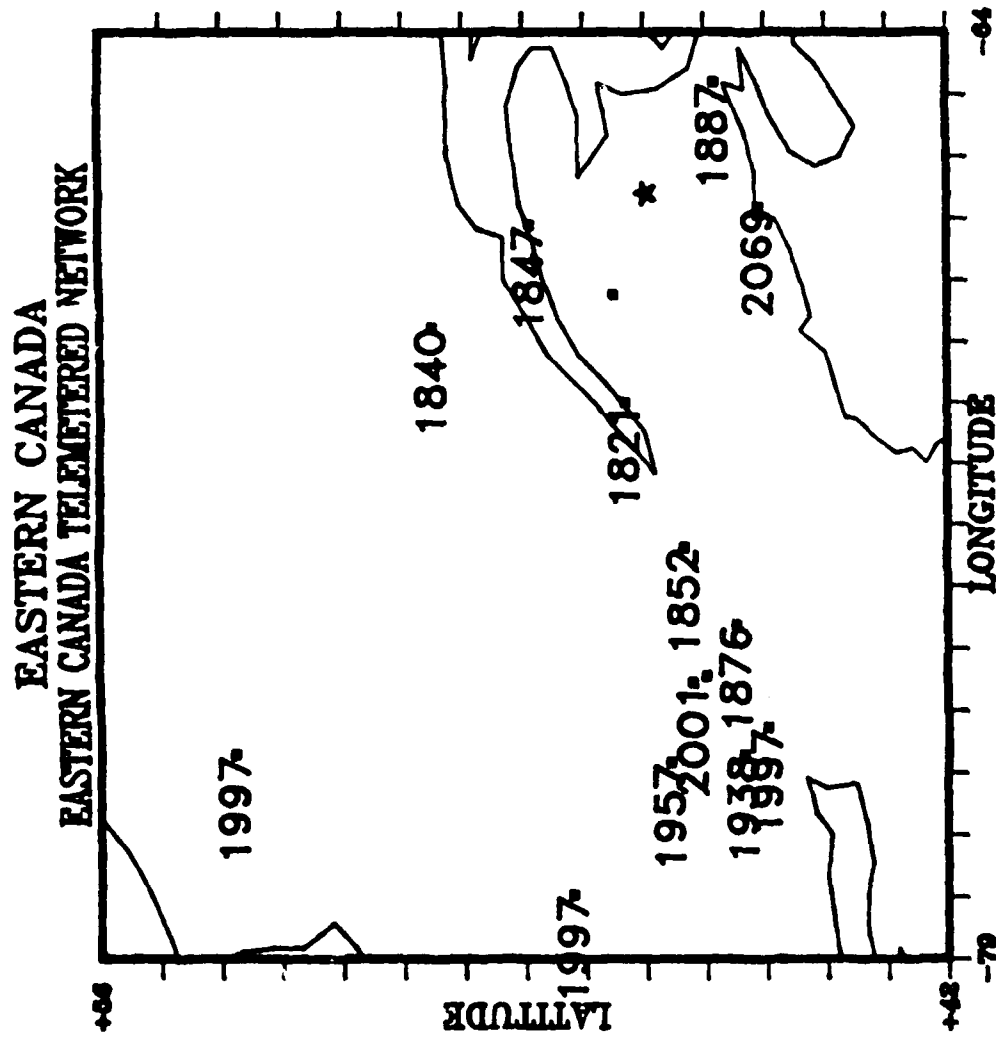


Fig. 8. Map showing the source region, star, and the high frequency Q determined for each station, which is plotted adjacent to the station location.

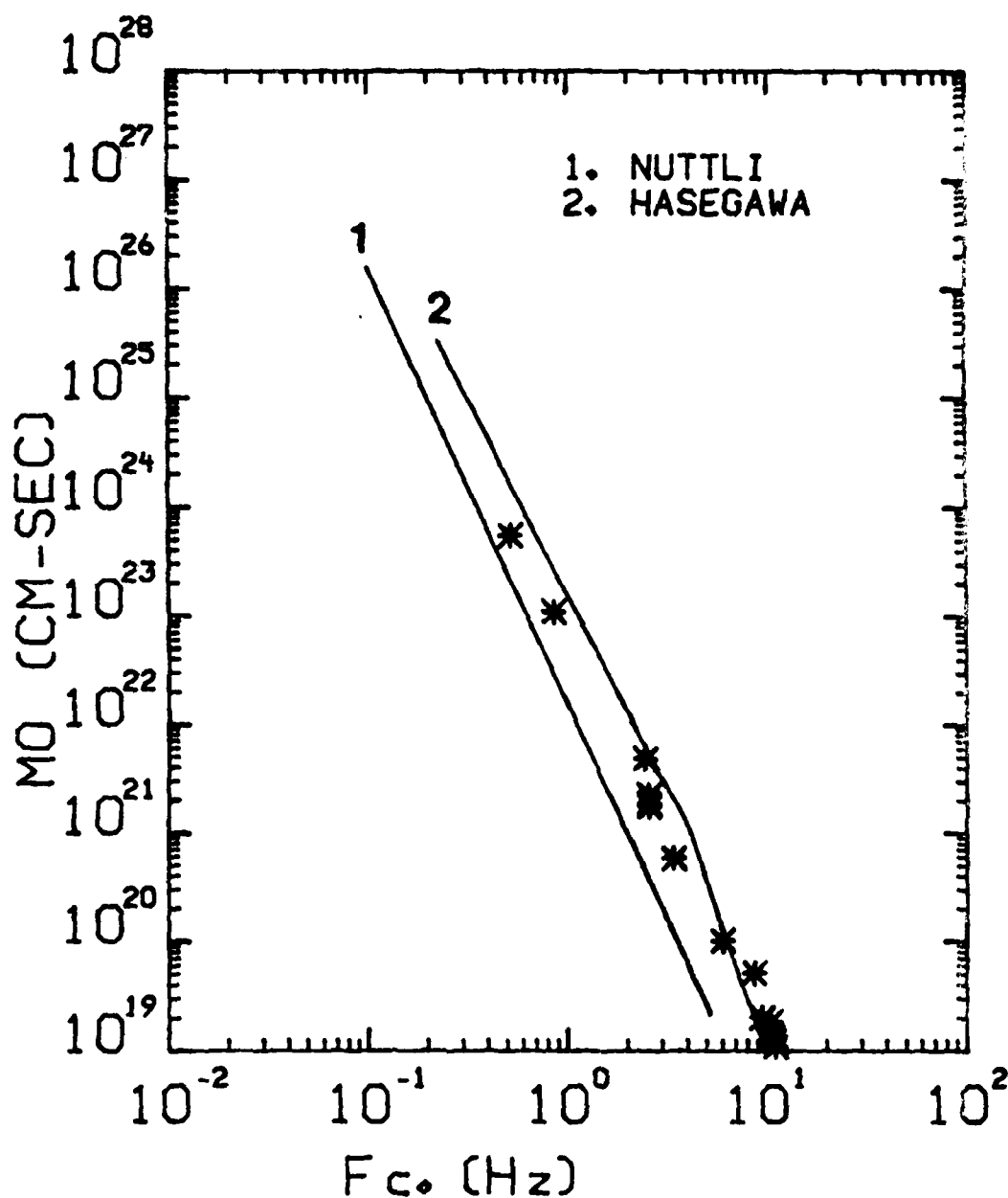


Fig. 9. Plot of Lg corner frequency, f_c , versus seismic moment, M_0 , for the events studied. The scaling laws proposed by Nuttli (1983) and Hasegawa (1983) are shown for comparison.

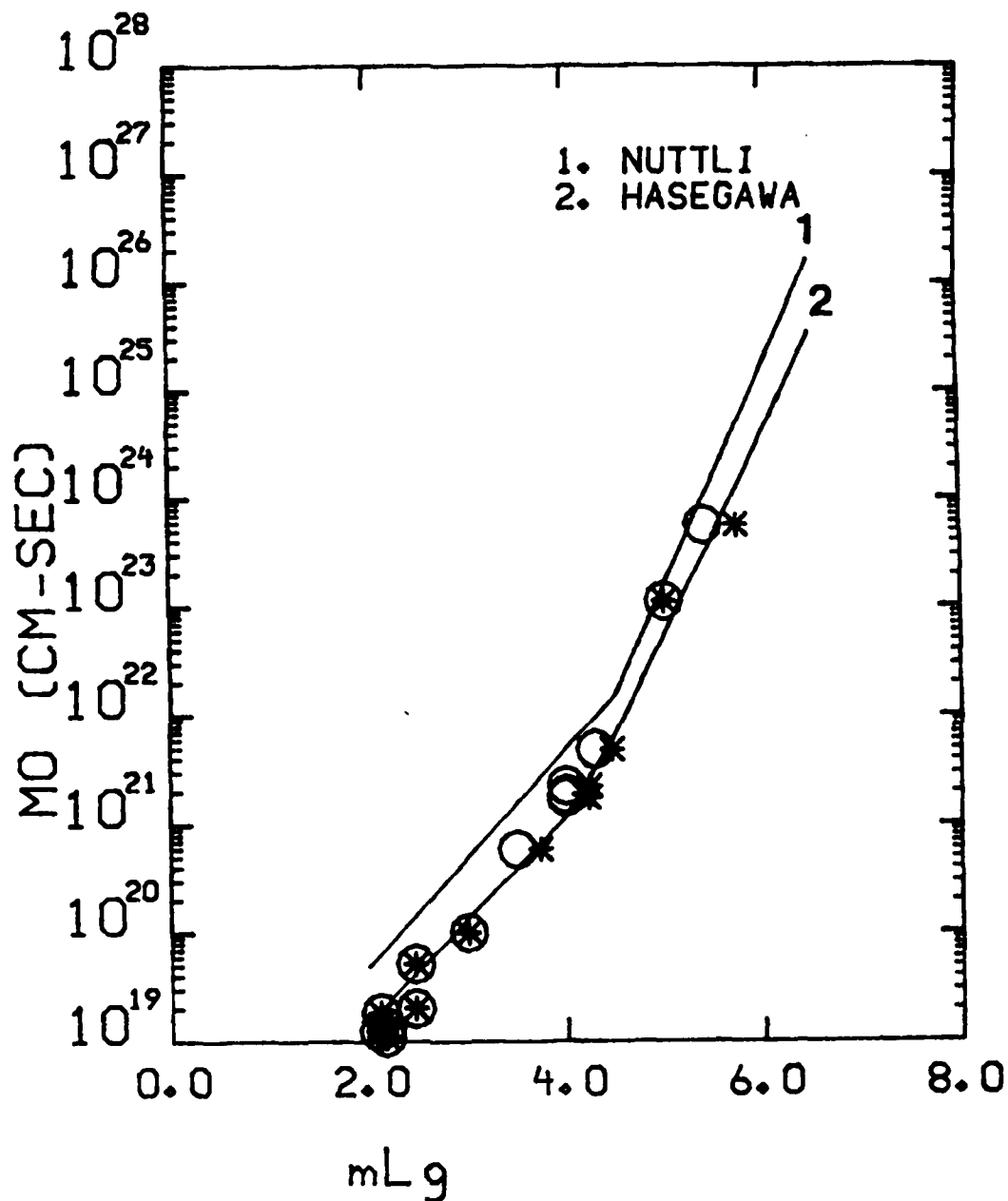


Fig. 10. Plot of seismic moment, M_0 , versus mLg . The circles are the ECTN catalog values and the asterisks are those determined in this study. In addition the Nuttli (1983) scaling law for mid-plate earthquakes and the Hasegawa (1983) relation for eastern Canada are given.

END

DTIC

7-86